Electron-Impact Excitation of the Argon Atom*

James K. Ballou and Chun C. Lin
Department of Physics, University of Wisconsin, Madison, Wisconsin 53706

Fredric E. Fajen
Mission Research Corporation, Santa Barbara, California 93102

(Received 9 April 1973)

Electron excitation functions of some thirty states of the $3p^5ns$, $3p^5np$, and $3p^5nd$ configurations of the argon atom have been measured by the optical method. In order to evaluate the level cross sections from the optical excitation cross sections, we have determined the branching ratios experimentally by measuring in an argon discharge tube the relative intensities of the emission lines originating from the level of interest. This procedure gives more accurate level cross sections than does the conventional approach of using theoretical transition probabilities to form the branching ratios, since for an atom as complex as argon the wave functions of the excited states calculated by a semiempirical treatment of the fine structure are not always of sufficient accuracy to give reliable transition probabilites. Analysis of the shape of the excitation functions is facilitated by expressing the wave functions of the excited states of argon in terms of the LS eigenfunctions, and the special features of the experimental data of excitation functions can be readily explained by generalizing the results of helium. Analogous to the case of neon, one can show theoretically that within a configuration $3p^5nl$, the states with odd values of $J + l$ in general have larger excitation cross sections than the ones with even values at incident energies well above the threshold, and that in general $Q(J = 0) > Q(J = 2)$, $Q(J = 1) > Q(J = 3)$ for the np states, and $Q(J = 1) > Q(J = 3)$, $Q(J = 2) > Q(J = 0,4)$ for nd. The experimental results of the excitation cross sections are found to be in good agreement with these rules.

I. INTRODUCTION

The study of electron excitation of the rare gases has played a very important role in understanding the nature of the electron-excitation processes of atoms.[1] The results of helium have provided a scheme for characterizing the shape of the excitation functions and magnitude of the cross sections of the various states in terms of the quantum numbers of the Russell-Saunders coupling scheme. The work on excitation of neon[2] has shown that application of this scheme can be extended to an atom like neon, which does not conform to LS coupling, provided that the wave functions of the excited states of this atom are expressed in terms of the LS eigenfunctions. In this manner Sharpton *et al.* were able to explain many of the qualitative features of the observed excitation functions and cross sections of some 50 states of neon.[2] Moreover, from theoretical considerations these authors have derived some qualitative relations between the magnitude of the cross sections of the levels within a configuration and the total angular momentum J of the excited states. With only a few exceptions, the experimental data are in accordance with the theoretical deduction.

We have extended the studies of electron excitation of the rare gases to the case of argon. In this paper we report our measurements of excitation functions of some 30 states of argon and analysis of the experimental data by means of the theoretical framework developed in Ref. 2. Most of the special features of the observed excitation data are found to conform, on a qualitative or even semiquantitative level, to the general theory. Through these comprehensive studies, we are now able to understand the results of a vast amount of experimental data of neon and argon in terms of a few underlying principles.

For the simple atoms, such as helium[3-5] and some of the alkali group,[6] considerable efforts have been put forth to compare the observed excitation cross sections with theoretical calculations based on first principles. With the availability of very accurate wave functions, good agreement between theory and experiment was found for only a limited number of states. In the case of the argon atom the complexity of the electron-electron interaction and of the coupling of the various angular-momentum vectors makes it very difficult to obtain highly accurate wave functions. While theoretical cross sections of argon can be calculated readily by using the Born approximation along with the Hartree-Fock-Slater-type wave functions (with the vector coupling treated by semiempirical means), as is done in this work, the accuracy of such theoretical values is believed to be much lower compared to the cases of helium and sodium. For this reason we shall not offer detailed discussion of comparison of

the magnitude of the measured excitation cross sections with the theoretical calculations. Instead, we are more concerned with understanding the qualitative and semiquantitative features of the experimental data from generalization of the results of helium and by simple theoretical considerations. The results of our theoretical calculations of the wave functions and excitation cross sections will be used in the analysis of experimental data mainly in a subordinate way.

II. METHOD OF MEASUREMENT

The experimental procedure for measuring electron-excitation cross sections by means of the optical method has been discussed in the literature.[1,5] Basically the first step is to measure the optical excitation cross sections of a transition ($j \rightarrow k$) originating from the particular excited state (j) of interest. In terms of the photon flux F_{jk} (per second) associated with the $j \rightarrow k$ transition produced by an electron beam of current I traversing through a length L of the gas, the optical cross section Q_{jk} is

$$Q_{jk} = F_{jk}(e/INL), \tag{1}$$

where e is the electronic charge, and N is the gas number density. The apparent cross section of the level j is obtained by summing all the optical cross sections corresponding to the downward transitions $j \rightarrow l$, i.e.,

$$Q^a(j) = \sum_{l<j} Q_{jl}. \tag{2}$$

For transitions originating from the same upper level j, the optical cross sections Q_{jl} are proportional to the transition probabilities $A(j \rightarrow l)$. Hence Eq. (2) can be rewritten as

$$Q^a(j) = Q_{jk} \sum_{l<j} \frac{A(j \rightarrow l)}{A(j \rightarrow k)}. \tag{3}$$

The apparent cross section of the level j therefore can be obtained by measuring the optical cross section of any one transition from j along with a knowledge of the various transition probabilities. The particular transition used for this purpose is generally chosen to be one of the stronger lines originating from j in the frequency range of photomultipliers. In most of the previous works theoretical transition probabilities were used in Eq. (3) to obtain the apparent cross sections. In the case of helium, for which accurate theoretical transition probabilities are available, this procedure proves to be quite adequate. However, the work of Sharpton *et al.* on neon has indicated that some of the theoretical transition probabilities of neon computed by the procedure described there may be subject to a sizable uncertainty, which greatly reduces the accuracy of the resulting apparent cross sections. The use of theoretical transition probabilities would most likely lead to even worse results for argon and therefore will not be adopted in this work.

An alternative procedure is to determine the relative transition probabilities from experiment. If we compare two transitions originating from the same upper level such as $j \rightarrow l$ and $j \rightarrow k$, their relative rate of photon emission is simply equal to the ratio of the two appropriate transition probabilities independent of the mechanism of population of the j level. In other words, we can obtain the ratio $A(j \rightarrow l)/A(j \rightarrow k)$ by measuring the intensities of the $j \rightarrow l$ and $j \rightarrow k$ transitions in a *discharge tube* in which the emission lines are much stronger than in an electron-beam collision chamber. In this manner we are able to take into account those lines ($j \rightarrow l$) which contribute substantially to $Q^a(j)$, but have frequencies in the low-sensitivity regions of the photon detectors, so that direct measurement of these lines in a collision chamber is difficult.

After obtaining the apparent cross sections, one seeks to ascertain the rate of population of the particular level due to cascade radiation. This may be accomplished by determining (from experimental measurements and/or theoretical inference) the optical cross sections of the transitions to the level in question from as many higher levels as one can. The level cross section $Q(j)$ is given by

$$Q(j) = Q^a(j) - \sum_{p>j} Q_{pj}. \tag{4}$$

In Fig. 1 is shown a block diagram of the apparatus for measuring optical excitation cross sections. Radiation emitted by the excited atoms in the electron-beam collision chamber is directed into the monochromator and detected by the photo-

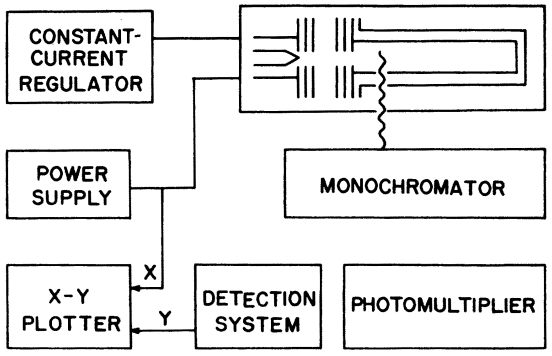

FIG. 1. Block diagram of the apparatus for measuring optical excitation cross sections.

multiplier. The output of the latter, after being processed by the detection system, is displayed in an X-Y plotter. The magnitude of the electron-beam current entering the Faraday cup is controlled by the grids and kept constant (with respect to the beam energy) by a feedback control system in which a corrective signal produced by the difference between the actual beam current and a fixed reference current is applied to the electron-gun control grid through an optical isolator. The inside wall of the Faraday cup was coated with Aquadag to reduce the production of secondary electrons. The length of the Faraday cup is about ten times the diameter of the entrance aperture, so that the bulk of both the incident electrons reflected and secondary electrons emitted by the end wall will reach the side wall without traversing through the region viewed by the monochromator. More detailed description of the electron gun and the detection system may be found in Ref. 7.

The experimental method for absolute measurements of photon flux has been described in Refs. 2 and 8. The optical excitation cross sections of argon were measured over a range of energy from threshold to 200 eV. For most of the lines reported in Table I, we have examined the light output as a function of the gas density. In several cases, notably for the lines originating from the $J=1$ and $J=2$ states of the $2p$ group, nonlinear dependence was observed at gas pressure as low as 2 mTorr. For such lines optical measurements were conducted at pressures about 1 mTorr (or less), resulting in rather low signal-to-noise ratio in the excitation functions. On the other hand, the light intensity is found to be quite linear with respect to the electron-beam current over the entire range of 20–100 μA used in this experiment.

An rf discharge tube with argon gas is used to measure the relative intensities of the lines originating from the same upper states for the $2p \rightarrow 1s$ and $4d \rightarrow 2p$ groups. The transition probabilities of many of these lines have been listed in the National Bureau of Standards publication *Atomic Transition Probabilities*.[9] Our values in most cases are in reasonable agreement with those of Ref. 9.

III. THEORY

The basic theory of electron excitation of neon has been treated in a previous paper.[2] The same general framework can be carried over to argon. We shall briefly indicate the key points of the theory in reference to its application to argon.

In describing the electronic structure of the atomic states, the one-configuration approximation is used. For a given configuration $2p^5nl$, the Hartree-Fock-Slater self-consistent-field method[10] is applied to compute the one-electron orbitals from which we construct the basis functions of the LS representation. Since the vector coupling between the various spin and orbital angular momenta is of the "intermediate" kind, the wave function of a state (of a given total angular momentum J) is expressed as a linear combination of the LS eigenfunctions of the same J. The coefficients of the LS eigenfunctions are determined by means of the method given by Cowan and Andrew[11] in which the values of the spin-orbit coupling constants and the Slater-Condon parameters are chosen so as to yield the best fit to the observed spacings of the energy levels of the configuration.

In discussing the qualitative behavior of electron excitation of the argon atom, we find it advantageous to express the wave functions of the excited states in the LS representation. As the excitation properties of a hypothetical LS state are known from Born-approximation considerations and/or the experimental results of the helium atom, by an appropriate superposition one can make theoretical predictions concerning the shape of the

TABLE I. Optical cross sections [a] (at maximum and at 100 eV) measured in units of 10^{-19} cm^2.

Transition	λ(Å)	Q_{ij} Max.	Q_{ij} 100 eV	Transition	λ(Å)	Q_{ij} Max.	Q_{ij} 100 eV
$2p_1$-$1s_2$	7503	97	64	$4s'_1$-$2p_{10}$	5912	2.2	2.1
$2p_5$-$1s_4$	7514	39	36	$4d_5$-$2p_{10}$	6871	5.5	1.4
$2p_3$-$1s_2$	8408	96	25	$4d_4$-$2p_8$	7353	5.0	1.6
$2p_6$-$1s_4$	8006	15	3.4	$4s''_1$-$2p_3$	7425	1.1	0.37
$2p_8$-$1s_4$	8424	122	32	$4d_3$-$2p_{10}$	6752	8.3	1.1
$2p_2$-$1s_2$	8265	24	9.7	$4s''_1$-$2p_{10}$	6059	1.1	0.10
$2p_4$-$1s_2$	8521	23	7.0	$4s''_1$''-$2p_4$	7412	1.6	0.17
$2p_7$-$1s_4$	8103	50	13	$4d_6$-$2p_{10}$	6937	3.0	0.23
$2p_{10}$-$1s_5$	9122	150	27	$4d'_4$-$2p_9$	7372	23	1.5
$2p_9$-$1s_5$	8115	260	11				

[a] See Sec. IV for experimental uncertainties of the optical cross sections.

excitation functions and the magnitude of the excitation cross sections for argon, at least on a qualitative level. For instance, the four LS eigenfunctions associated with the $3p^5 4s$ configuration are $\phi(^1P_1)$, $\phi(^3P_0)$, $\phi(^3P_1)$, and $\phi(^3P_2)$, whereas the actual atomic states of argon of this configuration (intermediate coupling) are designated as $1s_2(J=1)$, $1s_3(J=0)$, $1s_4(J=1)$, and $1s_5(J=2)$. Since the total angular momentum J remains a good quantum number, the wave functions of $1s_3$ and $1s_5$ are simply $\phi(^3P_0)$ and $\phi(^3P_2)$, respectively, and those of $1s_2$ and $1s_4$ are linear combinations of $\phi(^1P_1)$ and $\phi(^3P_1)$. One then expects the excitation functions of the $1s_3$ and $1s_5$ states to peak sharply near the threshold, similar to triplet excitation of helium. For the $1s_2$ and $1s_4$ states, because of the presence of the $\phi(^1P_1)$ component in their wave functions, the excitation functions *in general* should exhibit a very broad peak characteristic of the dipole-allowed states, and the excitation cross sections should be larger than those of $1s_3$ and $1s_5$ at energies well above the threshold. Exception to the preceding statement, however, may occur if the coefficient of the $\phi(^1P_1)$ term in the $1s_2$ or $1s_4$ wave function turns out to be very small. A similar analysis shows that the $2p_9$ state of $3p^5 4p$ and the $4d_6$ and $4d_4$ states of $3p^5 4d$ are purely triplet states with the characteristic narrow-peak excitation functions and that the $4d_5$, $4d_2$, and $4s_1'$ states (all $J=1$) *in general* may be expected to have broad peaks in their excitation functions.

To gain some insight to the magnitude of the cross sections of excitation from the ground state (i) to a final state (f), let us examine the Coulomb interaction of the six outer electrons of the atom (denoted by subscripts 1–6) with the colliding electron (denoted by subscript 7), or more specifically the coupling potential between the two states concerned, i.e.,

$$V_{fi}(7) = \int \psi_f^*(1,2,\ldots,6)\left(\sum_{j=1}^{6}\frac{1}{r_{j7}}\right) \times \psi_i(1,2,\ldots,6)\,d\vec{\tau}_1\ldots d\vec{\tau}_6 . \tag{5}$$

By means of an expansion of the type

$$\frac{1}{r_{17}} = \frac{1}{r_>}\sum_k \sum_{q=-k}^{k} \frac{4\pi}{2k+1}\left(\frac{r_<}{r_>}\right)^k \times Y_{kq}^*(\theta_7\phi_7)Y_{kq}(\theta_1\phi_1), \tag{6}$$

it can be shown that for a final state characterized by the configuration $3p^5 nl$ and the total angular momentum J, V_{fi} vanish if $J+l$ is even.[2] Under the nonexchange Born approximation, such a state would have zero excitation cross section; in other words, excitation occurs only through exchange effect and indirect coupling between i and f via some intermediate states. At high energies these effects are, in general, small compared to that due to nonvanishing direct coupling; thus one is led to the general conclusion that within a configuration $3p^5 nl$, the excitation cross sections of the states with odd values of $J+l$ as a whole are larger than those of the group of states with even $J+l$ at energies well above the threshold.

In reference to the specific case of the $3p^5 np$ configuration, the above rule leads to

$$Q(3p^5 np, J=0,2) > Q(3p^5 np, J=1,3). \tag{7}$$

Following the reasoning given in Ref. 2, one can further expect

$$Q(3p^5 np, J=0) > Q(3p^5 np, J=2), \tag{8}$$

because the coupling potential between the $3p^5 np$, $J=0$ state and the ground state ($J=0$) owes its origin to the first term ($k=0$) of the expansion in Eq. (6), whereas one must proceed to the $k=2$ term of the same expansion in order to obtain nonvanishing coupling of the $3p^5 np, J=2$ with the ground state. Both Eqs. (7) and (8) pertain to only the "high-energy" region, i.e., energies several times above the threshold. Likewise for the $3p^5 nd$ configuration we have

$$Q(3p^5 nd, J=1,3) > Q(3p^5 nd, J=0,2,4) \tag{9}$$

and

$$Q(3p^5 nd, J=1) > Q(3p^5 nd, J=3), \tag{10}$$

for high incident energies. The last inequality is based on the observation that the necessary coupling potentials for excitation of the $J=1$ and $J=3$ states (of $3p^5 nd$) are associated with, respectively, the $k=1$ and $k=3$ term of Eq. (6). It should be emphasized that the interpretation of (7)–(10) must be made with some care. For instance Eq. (8) indicates that the $J=0$ states *as a group* have larger cross sections than the $J=2$ state *as a group*, but does not mean that the cross section of *any one* of the $3p^5 np, J=0$ state is *always* larger than that of *any* of the $3p^5 np, J=2$. Possible exception on an individual basis may occur if a $J=0$ state, though normally consisting of a superposition of the $^1S_0$ and $^3P_0$ LS eigenstates, happens to have a very small weighting of the $^1S_0$ component and, as a result, unusually small cross sections. Among the states with even values of $J+l$ for which Eq. (6) gives no coupling, it was pointed out in Ref. 2 that one may expect the indirect-coupling effect to be much weaker for the purely triplet states than for the singlet-triplet mixed ones, resulting in smaller excitation cross sections for the former groups. Accordingly we may write

$$Q(3p^5np, J=1) > Q(3p^5np, J=3), \quad (11)$$

$$Q(3p^5nd, J=2) > Q(3p^5nd, J=0, 4). \quad (12)$$

Again the two preceding inequalities, strictly speaking, apply to the states inside the parentheses *as a group*. In dealing with cross sections of the individual levels, one should be aware of possible exceptions.

The electron-excitation cross sections were calculated by the Born approximation for the states which connect directly to the ground state through the coupling potential V_{if}. In the case of the purely triplet states, Ochkur's modification[12] of the Born approximation was employed. For the singlet-triplet mixed states with even values of $J+l$ that have zero potential coupling with the ground state, one may get nonvanishing cross sections by the use of Ochkur's procedure. However, the cross sections so obtained include only the exchange effect and fail to take into account the effect of indirect coupling through intermediate states. If the latter effect dominates the former as is often the case, such calculated cross sections would have little physical significance.

IV. RESULTS

Measurements of electron-excitation cross sections of argon have been reported by Fischer[13] and by Herrmann[14] in the 1930's and more recently by Volkova and Devyatov[15] and by Zapesochnyi and Feltsan.[16] We found rather substantial differences in the shape of excitation functions between the results of Herrmann[14] and of this work, and the peak excitation cross sections in some cases differ by a factor greater than 2. Likewise, our excitation data of the $3p$ states show significant discrepancy from those of Fischer.[13] Because of the difference in the experimental methods used by Fischer and by Herrmann from ours, no detailed comparison of these three groups of data will be made. Our peak cross sections (apparent) of the $2p$ states agree to within about 20% with those of Zapesochnyi and Feltsan[16] with the exception of the $2p_4$, $2p_9$, and $2p_{10}$ states, where a difference ranging from 40% to a factor of 2 was found. Compared to the data of Volkova and Devyatov,[15] our peak optical cross sections for a number of $2p-1s$ lines are, in general, considerably larger than the corresponding effective cross sections given in Ref. 15. It may be noted that for detecting the atomic radiation, photographic films were used by Volkova and Devyatov,[15] whereas photoelectric recording was adopted in the work of Zapesochnyi and Feltsan.[16]

For the purpose of comparison of our experimental data with those obtained from other laboratories, we have measured the excitation cross sections of the 4806- and 4579-Å lines of Ar^+ and the 5852- and 5945-Å lines of Ne. In all cases our results agree to within 15% or better with those of Latimer and St. John[17] (He^+) and of Sharpton *et al.*[2] (Ne).

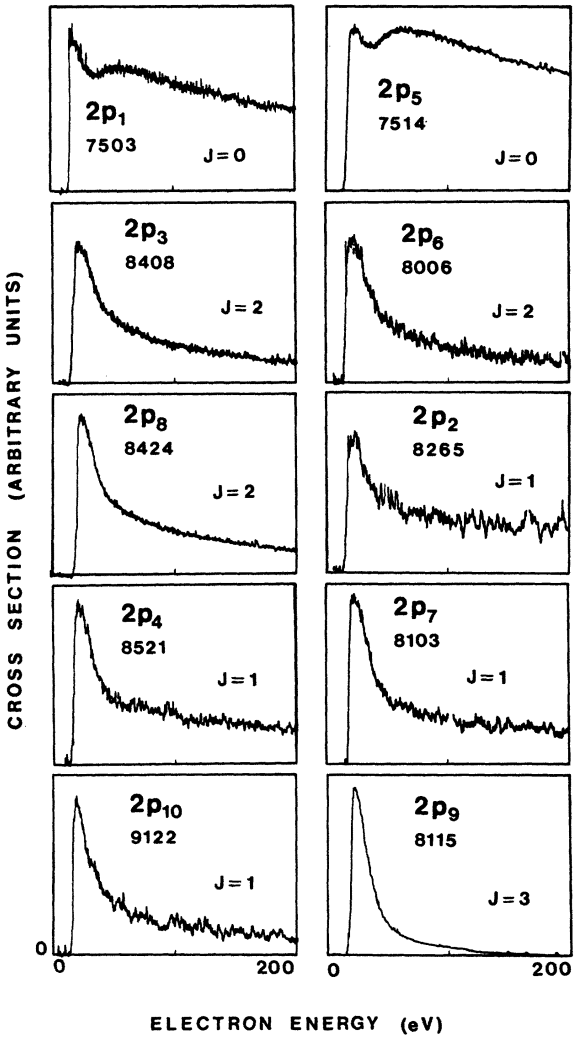

FIG. 2. Optical excitation functions of the $2p$ states.

No polarization of the observed radiation was found; hence, the intensity of the atomic radiation was treated as being isotropic in the reduction of experimental data. The experimental uncertainty of a typical optical cross section is about 15%, but may become twice as large when the magnitude of the cross section is below 0.2×10^{-19} cm^2.

A. $2p$ and $3p$ Families

The optical excitation functions of the ten $2p$ levels of argon are displayed in Fig. 2. Several special features are readily recognizable. The $2p_9$ state, which is a pure $^3D_3$ state, exhibits a

narrow excitation function characteristic of a triplet state. The two $J=0$ states ($2p_1$ and $2p_5$) have distinctly broader excitation functions than all the others. (The narrow spikes at 20 eV will be discussed in the next paragraph.) In comparing the excitation functions of the $J=0$ states with those of the $J=2$ states, one may recall that from the theoretical viewpoint, the coupling potentials connecting the ground state with the $J=0$ states and with the $J=2$ states can be traced to the $k=0$ and the $k=2$ terms, respectively, in the expansion of Eq. (6). For the case of helium the $k=0$ terms are responsible for the excitation of the ^1S states and the $k=2$ terms for ^1D. Examination of the experimental excitation data of helium shows the ^1S excitation functions to have a slower decline with increasing energy than the ^1D functions.[5] Thus we see a parallel analogy between argon and helium in this respect. As for the $J=1$ states, the coupling potentials connecting them with the ground state vanish, and the cross sections are attributed to exchange and indirect-coupling effects. The excitation functions would have a very narrow shape if the exchange effect completely dominated the indirect coupling, but would become broader as the indirect-coupling effect began to play a more important role. We see from the experimental data that the curves of the $J=1$ states are much broader than that of the pure triplet state $2p_9$. In fact, there appears to be no gross difference between the $J=1$ and the $J=2$ groups as far as the general width of the excitation functions is concerned, except for the $2p_{10}$ state, which does have a distinctly narrower excitation function than all the other $J=2$ members. Thus from a comparison of the shape of the excitation functions, one can recognize the importance of indirect couplings in determining excitation cross sections.

Another interesting feature is that both the $2p_1$ and $2p_5$ curves show a narrow peak at about 20 eV before reaching the broad maximum. The same double-peak feature is also found in the cases of $3p_1$, $3p_5$, $4p_1$, and $4p_5$. One may wonder if the low-energy narrow peak may be due to cascade from some tripletlike levels. However, the purely triplet states of the $3p^5ns$ and $3p^5nd$ configurations have $J=0,2$ and $J=0,4$, respectively; none of these states are capable of dipole-radiative cascade to $2p_1$ and $2p_5$ ($J=0$). Although some of the $J=1$ states (e.g., $4d_5$), which are optically allowed with respect to $2p_1$ and $2p_5$, accidentally have very steep descending excitation functions (see Sec. IV B), it is very unlikely that cascade from such states can account for the sharp peak near the onset of the excitation functions of all the $2p_1$, $2p_5$, $3p_1$, $3p_5$, $4p_1$, and $4p_5$ states. One possible explanation is that the wave functions of the $2p_1$ and $2p_5$ states consist of linear combinations of the LS eigenfunctions of $^3P_0$ and $^1S_0$; the sharp-peak contribution of the $^3P_0$ component, when added to a rather broad excitation function, produces a noticeable peak near the onset. However, this is merely a speculation, as we have not investigated it in any quantitative way.

The optical cross sections of the ten lines exhibited in Fig. 2 are included in Table I. The cross sections of all the other $2p \rightarrow 1s$ lines can then be determined by adopting the procedure described in Sec. II, and are presented in Table II. In Table III are given the apparent cross sections of the ten $2p$ states. The $2p$ levels are subject to cascade from the $3p^5ns$ and $3p^5nd$ groups. We have measured the cascade contributions from the $3p^56s$, $3p^57s$, $3p^54d$, and $3p^55d$ configurations and found only the $3p^56s$ and $3p^54d$ cascades to be of any appreciable importance. Corrections due to these cascade effects have been made to the apparent excitation cross sections of the $2p$ states. Cascades from higher configurations are estimated to be entirely negligible. The transitions from the $3p^55s$ and $3p^53d$ to the $2p$ levels are in the infrared region, and we are not able to detect

TABLE II. Optical cross sections (Q_{ij}) of the $2p \rightarrow 1s$ and $4d \rightarrow 2p$ lines at 100 eV in units of 10^{-19} cm^2.

	$2p_1$	$2p_2$	$2p_3$	$2p_4$	$2p_5$	$2p_6$	$2p_7$	$2p_8$	$2p_9$	$2p_{10}$
$1s_2$	64	9.7	25	7.0	0	5.4	0.83	4.4	0	0.29
$1s_3$	0	4.3	0	5.9	0	0	2.0	0	0	2.2
$1s_4$	0	0.92	8.7	0.013	36	3.4	13	32	0	15
$1s_5$	0	3.1	4.3	0.19	0	17	2.6	16	11	27
$4d_4$	0	0	0	0	0	0.11	0	1.6	0.18	0
$4s'_1$	0	0	0.37	0	0	0.16	0	0.41	0.13	0
$4d_3$	0	0	0	0	0	0	0.068	0	0.58	1.1
$4s''_1$	0	0.07	0.1	0.01	0	0.05	0.05	0	0.06	0.10
$4s'''_1$	0	0.08	0	0.17	0	0.1	0.06	0.05	0.003	0.05
$4d_6$	0	0	0	0	0	0	0.06	0	0	0.23
$4d'_4$	0	0	0	0	0	0	0	0	1.5	0

any of these lines in our collision-chamber experiment. However, if we take the ratio of the theoretical excitation cross sections of the $3p^5 5s$ states to those of the $3p^5 6s$ states as a measure of the ratio of the $3p^5 5s \rightarrow 3p^5 4p$ cascade to the $3p^5 6s \rightarrow 3p^5 4p$ cascade, and adopt a similar criterion for the $3p^5 3d \rightarrow 3p^5 4p$ vs $3p^5 4d \rightarrow 3p^5 4p$ cascade, we estimate the cascade from the $3p^5 5s$ and $3p^5 3d$ states to be less than 15% of the apparent cross sections for all the $2p$ states at 100 and 200 eV, except $2p_{10}$ (at 200 eV), and $2p_3$, $2p_4$, $2p_9$ (at both 100 and 200 eV), for which this cascade contribution may constitute as much as 24–30% of the total population. However, in view of the lack of experimental data of the optical cross sections of the $3p^5 5s \rightarrow 3p^5 4p$ and $3p^5 3d \rightarrow 3p^5 4p$ transitions, corrections for these cascade transitions were not made in our data. In other words, the level cross sections of the $2p_{10}$ at 200 eV and of $2p_3$, $2p_4$, $2p_9$ at both 100 and 200 eV given in Table III may represent an overestimation by as much as 25–30%.

From Table III it is seen that with the exception of the $2p_{10}$ state, all the even-J states of the $2p$ group have larger cross sections than do the odd-J ones at 100 and 200 eV. The cross sections of the $2p_{10}$ decreases very rapidly with energy. Thus at 100 eV the $2p_{10}$ cross section is well above those of $2p_3$ and $2p_6$, but becomes equal to the $2p_6$ value (the smallest of all $J=2$ states) when the incident energy is raised to 200 eV. With increasing incident energies, one may expect the $2p_{10}$ cross sections to drop below those of all the $J=2$ states. Among the even-J states, the cross sections of the $J=0$ states ($2p_1$ and $2p_5$) are larger than those of the $J=2$ states ($2p_3$, $2p_6$, $2p_8$) at 200 eV, although at 100 eV the $2p_8$ cross section exceeds the $2p_5$ value. For the states with odd values of J, the purely triplet $2p_9$ state ($J=3$) has lower cross sections than the $J=1$ states. These results are in good agreement with the predictions of the theoretical considerations given in Sec. III.

The theoretical cross sections of the $J=0$ and $J=2$ states calculated by means of the Born approximation are included in Table III. For the $J=1$ states the use of the Born approximation (with Ochkur's modification) is unrealistic because the effects of indirect coupling are not taken into consideration. For this reason no theoretical values of the cross sections of the $J=1$ states are given. While the theoretical cross sections of the $J=0$ states agree reasonably well with experiment, a discrepancy of a factor of 3 to 8 is seen between theory and experiment for the $J=2$ states. This discrepancy is of comparable magnitude to the corresponding one for Ne.[2] The Ochkur modification of the Born approximation was employed to calculate the excitation cross sections of the purely triplet state $2p_9$. The theoretical values are found to be more than an order of magnitude smaller than the experimental data.

We have measured the excitation functions of all the $3p$ states except $3p_7$ and $3p_3$. The two stronger lines of the $3p_7 \rightarrow 1s$ group (4272 and 4164 Å) are contaminated by Ar^+ lines at nearly the same wavelengths, and the two other lines are too weak to measure in our apparatus. As for the $3p_3$ state, all the three allowed $3p_3 \rightarrow 1s$ lines have neighbor-

TABLE III. Experimental values of the apparent and level cross sections of the $2p$ states at 100 and 200 eV and comparison with the theoretical level cross sections in units of 10^{-19} cm^2.

		100 eV			200 eV		
States	J	Expt.[a] App. Q	Expt.[b,c] Level Q	Theor.[b] Level Q	Expt.[a] App. Q	Expt.[b,c] Level Q	Theor.[b] Level Q
$2p_1$	0	64	63	82.4	48	48	43.1
$2p_5$	0	36	35	18.2	28	28	9.6
$2p_3$	2	38	33	6.0	22	19	3.2
$2p_6$	2	26	24	7.4	14	13	4.0
$2p_8$	2	52	48	6.4	27	24	3.4
$2p_2$	1	18	16		12	11	
$2p_4$	1	13	11		8.8	7.8	
$2p_7$	1	18	17		12	11	
$2p_{10}$	1	44	39		16	13	
$2p_9$	3	11	9	0.33	2	2	0.04

[a] Here "App. Q" refers to "apparent cross sections," as defined by Eq. (2). The experimental uncertainty is about 15%.

[b] Here "Level Q" refers to "level cross sections," as defined by Eq. (4).

[c] In addition to the estimated 15%, the uncertainty of the experimental level cross sections contains the error due to neglecting cascade from the $3p^5 5s$ and $3p^5 3d$ groups. See Sec. IV A for an estimate of this error.

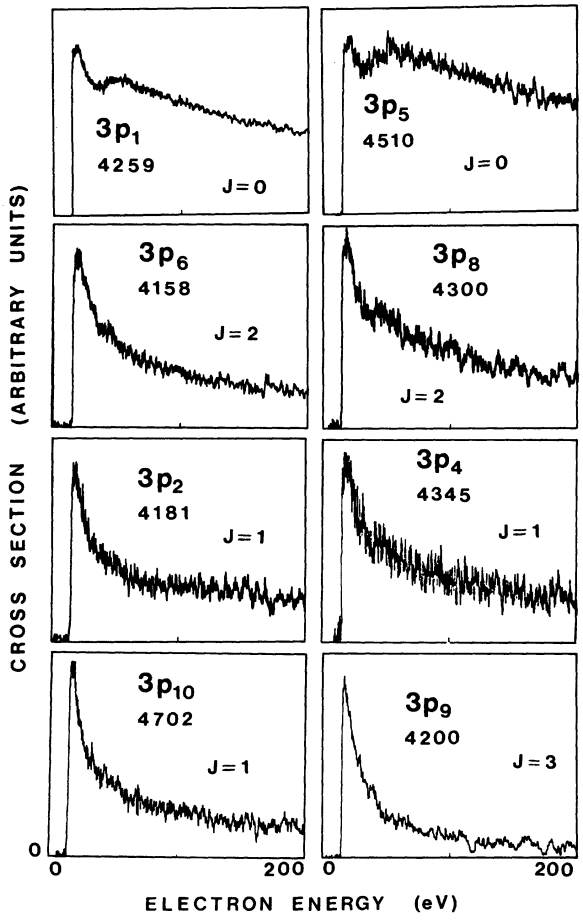

FIG. 3. Optical excitation functions of the $3p$ states.

ing lines (from the $3p_2$ state) within 2 Å. The shapes of the excitation functions of the eight $3p$ states shown in Fig. 3 are similar to their counterparts in the $2p$ series. In order to evaluate the apparent excitation cross sections it is necessary to determine the relative transition probabilities of the $3p \rightarrow 1s$, $3p \rightarrow 3d$, and $3p \rightarrow 2s$ transitions. The last two groups of lines are in the infrared region, and because of the lower detection sensitivity achievable in the infrared compared to the visible range, we have not been successful in observing any of the $3p \rightarrow 3d$ and $3p \rightarrow 2s$ lines in the discharge tube. Without a knowledge of the branching ratios, we are unable to determine the apparent excitation cross sections and therefore will not endeavor to discuss the quantitative aspects of the excitation behaviors of the $3p$ states.

B. $4d$ Family

The optical excitation functions of nine of the twelve states of the $3p^5 4d$ configuration are displayed in Fig. 4 and the optical excitation cross sections may be found in Table I; spectral lines originating from the other three states ($4d_2$, $4d_1''$, and $4d_1'$) are too weak to detect in our collision apparatus. The $J=1$ states of the $3p^5 nd$ configuration are expected to give rise to very broad excitation functions typical of the dipole-allowed states. The experimental data of the $4d_5$ state, however, are in contradiction with our expectation (Fig. 4). The explanation lies in the wave function of the specific state concerned. Within the $3p^5 nd$

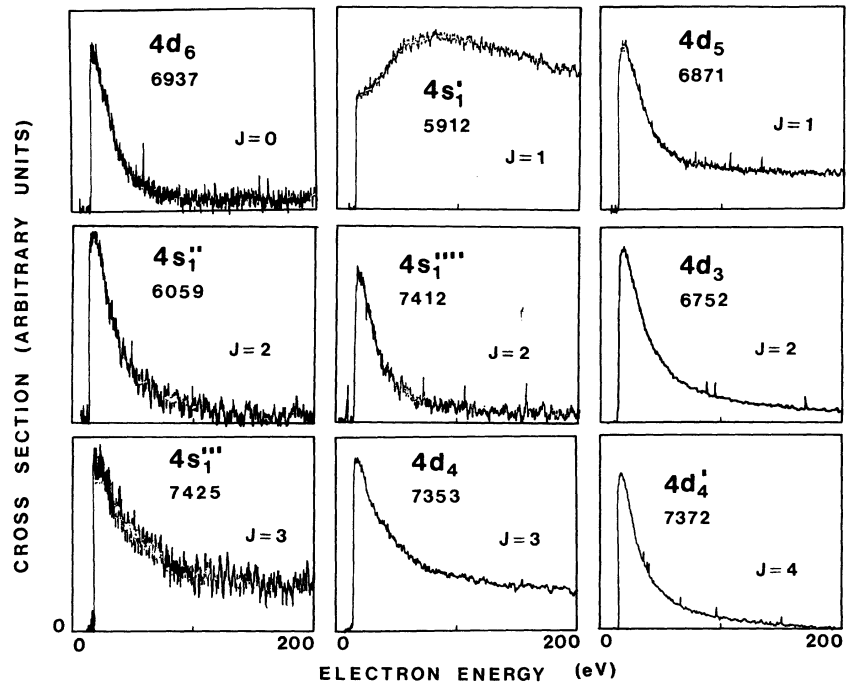

FIG. 4. Optical excitation functions of the $4d$ states.

configuration a state with $J=1$ consists of a superposition of three LS eigenstates, i.e., $^1P_1$, $^3P_1$, and $^3D_1$, and our intermediate coupling calculations give the coefficients of these three LS components in the wave function of the $4d_5$ state as 0.120, −0.975, and 0.186, respectively. The contribution to the excitation function of the $4d_5$ state from the $^1P_1$ component, which is responsible for the broad peak, is overshadowed by that from $^3P_1$, resulting in a tripletlike curve.

The $4d_6$ and $4d_4'$ are both pure triplet states ($^3P_0$ and $^3F_4$, respectively), and do indeed exhibit the usual narrow excitation function. It is interesting to note that the three $J=2$ states ($4s_1''$, $4d_3$, $4s_1''''$) have considerably narrower excitation functions than do the $J=3$ states. In particular, the excitation functions of the $4s_1''$ and $4s_1''''$ states have about the same shape as those of the two purely triplet states. We may recall from the general theory described in Sec. III that the direct potential coupling of the ground state with the $J=2$ states of the $3p^5nd$ configuration vanishes, and excitation of the latter states is caused by exchange and indirect-coupling effects. Exchange effect alone would give rise to a tripletlike excitation function, and inclusion of indirect coupling has the result of broadening that curve. The experimental data in Fig. 4 are suggestive of relatively small indirect-coupling effect on the cross sections of the $4s_1''$ and $4s_1''''$ states, but appreciably larger for $4d_3$. However, even with the aid of indirect coupling, the excitation functions of the $J=2$ states do not turn out to be as broad as those of the $J=3$ states, for which direct coupling with the ground state exists through the $k=3$ term of Eq. (6). This is in contrast to our observations for the $2p$ group, where the $J=1$ states (which have no direct potential coupling with the ground state and therefore are the counterpart of the $J=2$ states of the $4d$ group) and the $J=2$ states (which connect directly with the ground state corresponding to the $3p^54d$, $J=3$ states) have excitation functions of very similar shape.

The principal depopulation mechanism of the $4s_1'$ state is expected to be the transition to the ground state (830 Å). Since our experimental apparatus is not equipped to handle vacuum-ultraviolet radiation, we are unable to determine the apparent excitation cross sections of the $J=1$ states. The other $4d$ states make radiative transitions to $2p$ and $3p$. The $4d\rightarrow 2p$ lines are in the spectral region of 5900–9100 Å; their relative intensities were readily determined from our discharge experiment. However, we are not able to observe any of the $4d\rightarrow 3p$ lines (above 25000 Å). In view of their long wavelengths it is probable that the $4d\rightarrow 3p$ lines, in general, have smaller transition probabilities than the $4d\rightarrow 2p$ lines, and in the absence of experimental data on the transition probabilities of the $4d\rightarrow 3p$ lines, we shall neglect them in computing the branching ratios in Eq. (3). The apparent excitation cross sections of the $4d$ states as given in Table IV are therefore subject to a higher degree of uncertainty than those of the $2p$ states. In Table II we give a breakdown of the individual optical cross sections of the relevant $4d\rightarrow 2p$ lines, which were obtained by means of the method described in Sec. II, along with the cross sections in Table I.

Determination of the cascade contribution to the $4d$ states is again complicated by the fact that all the transitions terminating at $4d$ have frequencies in the infrared region. Nevertheless, to ascertain the importance of the cascade from the $4p$ states, we have examined the optical excitation cross sections of the $4p\rightarrow 1s$ transitions. The only lines from this group that we can detect in our electron-beam experiment originate from $4p_1$ and $4p_5$ (both $J=0$), which cascade only to the $J=1$ states of $3p^54d$, but not to the states listed in Table IV. For all the other $4p\rightarrow 1s$ (except $4p_1$ and $4p_5$) lines, we can place an upper limit on the cross sections at 100 eV as 3×10^{-21} cm^2. Of course we do not have a good estimate of the transition probabilities of $4p\rightarrow 1s$ relative to $4p\rightarrow 4d$. In view of the fact that $l\rightarrow l+1$ cascade is usually less favorable than $l\rightarrow l-1$, and in view of the low frequencies of the $4p\rightarrow 4d$ transitions, it is not likely that these lines have sufficiently large transition probabilities to make significant cascade contributions to the $4d$ states. Another source of cascade is from

TABLE IV. Experimental values of the apparent excitation cross sections of the $4d$ states at 100 and 200 eV and the theoretical level cross sections in units of 10^{-19} cm^2.

		100 eV		200 eV	
		Expt.[a]	Theor.[b]	Expt.[a]	Theor.[b]
States	J	App. Q	Level Q	App. Q	Level Q
$4d_4$	3	1.9	1.6	1.3	0.82
$4s_1''$	3	1.1	3.4	0.8	1.7
$4d_3$	2	1.8		0.8	
$4s_1'$	2	0.4		<0.1	
$4s_1'''$	2	0.5		≤0.3	
$4d_6$	0	0.3	0.11	<0.3	0.013
$4d_4'$	4	1.5	0.31	<0.1	0.039

[a] Here "App. Q" refers to "apparent cross sections," as defined by Eq. (2). The experimental uncertainty of these cross sections is larger than the 15%–30% range stated in Sec. IV because the transition probabilities of the $4d\rightarrow 3p$ lines were neglected in computing the branching ratios.

[b] Here "Level Q" refers to "level cross sections," as defined by Eq. (4).

the $3p^5nf$ states; however, we are unable to detect any emission lines from these states in our excitation experiment. Our theoretical calculations give excitation cross sections of all three $4p^54f$, $J=2$ states as about 1×10^{-20} cm^2 at 100 eV and much smaller (by an order of magnitude or more) cross sections for all other members of the same configuration. Each $4p^54f, J=2$ state may cascade to a total of 14 states of the $4p^53d$ and $4p^54d$ configurations; thus one would expect the $4f$-cascade contribution to the apparent cross sections of the $4d$ states listed in Table IV to be quite small. For the reasons described in this paragraph, we shall take the apparent excitation cross sections of Table IV as being approximately equal to the level cross sections.

Inspection of Table IV reveals that the experimental cross sections for the $J=3$ states as a group are larger than the ones for the even-J states, as expected from theoretical grounds. When an examination of each individual state is made, we do notice an exception in that the $4d_3$ cross section is larger than the $4s_1''$ one at 100 eV. However, at 200 eV the cross sections of these two states become equal to each other; thus at higher energies we expect the $4d_3$ cross sections to drop below $4s_1''$, since the excitation function of the $4d_3$ state declines more steeply with energy than its $4s_1''$ counterpart. Among the even-J states we again find good accordance between theory and experimental results, in that the $J=2$ states collectively have larger cross sections than do the two purely triplet states ($J=0,4$) at 200 eV. Comparison on an individual basis in this case is made difficult because of the large degree of uncertainty of the cross sections for most of the even-J states at 200 eV. Of some interest is the observation that the $4d_3$ state has a much larger cross section than the other two $J=2$ states in Table IV. Since the $J=2$ states do not couple directly with the ground state through Coulomb interaction, our experimental data here suggest that the indirect-coupling effect is much more prominent in the $4d_3$ state than in $4s_1'$ and $4s_1''$. It may be recalled that the same conclusion was obtained by consideration of the shape of the excitation functions.

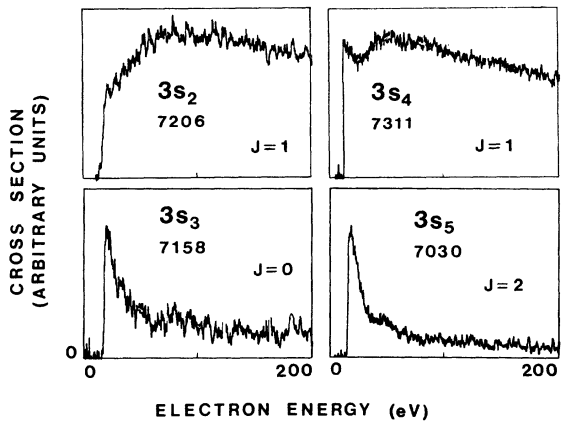

FIG. 5. Optical excitation functions of the 3s states.

Theoretical level cross sections calculated by the Born approximation (with Ochkur's modification for the purely triplet states) are included in Table IV. The over-all agreement between the theoretical and experimental values is seen to be reasonably satisfactory.

C. 3s Family

The optical excitation functions of the four $3s$ states are shown in Fig. 5. As may be expected, narrow excitation functions are found for the purely triplet states $3s_3$ and $3s_5$, whereas the $3s_2$ and $3s_4$ states ($J=1$) show the broader peak characteristic of the dipole-allowed states. No attempt has been made, however, to evaluate the apparent excitation functions due to the lack of experimental data of the transition probabilities of the $3s\rightarrow3p$ lines and especially the emission lines from $3s_2$ and $3s_4$ to the ground state.

V. SUMMARY AND CONCLUSIONS

The qualitative features of the excitation functions of the levels of the $3p^5ns$, $3p^5np$, and $3p^5nd$ configurations reported in this paper can be explained by generalizing the results observed for helium along with a general theoretical consideration developed in an earlier paper on neon. Within a given configuration $3p^5nl$, the states with odd values of $J+l$ are found to have larger cross sections than the even-$(J+l)$ states at incident energies well above the excitation threshold. Furthermore, it was observed that in general $Q(J=0)>Q(J=2)$ and $Q(J=1)>Q(J=3)$ for the np states, and $Q(J=2)>Q(J=0,4)$ for nd. These observations are in good agreement with the predictions of theory. Calculations of the excitation cross sections have been made of the odd-$(J+l)$ states by means of the Born approximation based on Hartree-Fock-Slater-type wave functions (with a semiempirical treatment of the fine-structure vector coupling). The discrepancy between the calculated and experimental values ranges from 24% ($2p_1$) to a factor of 8 ($2p_8$) for the $2p$ states, and from 20% to a factor of 3 for $4d$. The degree of discrepancy shown here is of comparable magnitude to that found in neon. It is felt that the disagreement between theory and experiment is to a large measure due to the inaccuracy of the wave functions, particularly the semiempirical method for determining the

coefficients of expansion of the wave functions in terms of the LS eigenfunctions.

To convert the measured optical excitation cross sections into the apparent cross sections, it is customary to multiply the former by the appropriate branching ratios obtained from the theoretical transition probabilities. For atoms with complex structure like neon, the use of the theoretical transition probabilities may result in a rather large uncertainty in some of the apparent excitation cross sections. In this paper we have eliminated this source of inaccuracy by determining the branching ratios experimentally from measurements of relative intensities in an argon discharge tube. Since in our laboratory we are not equipped for vacuum-ultraviolet work and the detection sensitivity at wavelengths above 10 000 Å decreases markedly, we were not able to measure the relative intensities for all the lines necessary to obtain the branching ratios of a number of states, notably the $3p$ and $3s$ groups. To use the optical method effectively for determining excitation cross sections, it should be very desirable to extend the frequency range of sensitive detection to both vacuum ultraviolet and the entire infrared region.

The results of this work and Ref. 2 have provided us with a simple scheme to describe electron-excitation processes of noble gases which enables us to understand most of the qualitative and semiquantitative features of the experimental data of excitation cross sections of some 30 states of argon and 60 states of neon.

---

*Research supported in part by the Air Force Office of Scientific Research, Office of Aerospace Research, U.S. Air Force.

[1]See, for example, B. L. Moiseiwitsch and S. J. Smith, Rev. Mod. Phys. **40**, 238 (1968).

[2]F. A. Sharpton, R. M. St. John, C. C. Lin, and F. E. Fajen, Phys. Rev. A **2**, 1305 (1970).

[3]M. Inokuti, Rev. Mod. Phys. **43**, 297 (1971).

[4]S. Chung and C. C. Lin, in *Proceedings of the Sixth International Conference on the Physics of Electronic and Atomic Collisions: Abstracts* (MIT Press, Cambridge, Mass., 1969), p. 363.

[5]R. M. St. John, F. L. Miller, and C. C. Lin, Phys. Rev. **134**, A888 (1964).

[6]D. F. Korff, S. Chung, and C. C. Lin, Phys. Rev. A **7**, 545 (1973).

[7]R. J. Anderson, E. T. P. Lee, and C. C. Lin, Phys. Rev. **157**, 31 (1967).

[8]R. M. St. John, *Methods of Experimental Physics* (Academic, New York, 1969), Vol. 8, p. 27.

[9]W. L. Wiese, M. W. Smith, and B. M. Miles, *Atomic Transition Probabilities*, Natl. Bur. Stand. (U.S.), Nat. Stand. Ref. Data. Ser.-22 (U.S. GPO, Washington, D. C., 1969), Vol. II.

[10]F. Herman and S. Skillman, *Atomic Structure Calculations* (Prentice-Hall, Englewood Cliffs, N.J., 1963).

[11]R. D. Cowan and K. L. Andrew, J. Opt. Soc. Am. **55**, 502 (1965).

[12]V. I. Ochkur, Zh. Eksp. Teor. Fiz. **45**, 734 (1963) [Sov. Phys.-JETP **18**, 503 (1964)].

[13]O. Fischer, Z. Phys. **86**, 646 (1933).

[14]O. Herrmann, Ann. Phys. (Leipz.) **25**, 143 (1936).

[15]L. M. Volkova and A. M. Devyatov, Opt. Spektrosk. **7**, 819 (1959) [Opt. Spectrosc. **7**, 480 (1959)].

[16]I. P. Zapesochnyi and P. V. Feltsan, Opt. Spektrosk. **20**, 521 (1966) [Opt. Spectrosc. **20**, 291 (1966)].

[17]I. D. Latimer and R. M. St. John, Phys. Rev. A **1**, 1612 (1970).